Journal of Sound and Vibration (1997) **202**(1), 95–108

SURFACE MOBILITY OF A CIRCULAR CONTACT AREA ON AN INFINITE PLATE

C. NORWOOD

Ship Structure and Materials Division, AMRL, Defence Science and Technology Organisation, P.O. Box 4331, *Melbourne, Victoria, Australia*

AND

H. M. WILLIAMSON AND J. Y. ZHAO

Acoustics and Vibration Centre, University College, The University of New South Wales, Australian Defence Force Academy, Canberra, Australia

(*Received* 7 *March* 1996, *and in revised form* 18 *September* 1996)

Theoretical models for surface mobility are derived using two alternative approaches: time averaged input power and effective mobility. The surface mobility of a circular contact area of an infinite plate is investigated for both uniform conphase contact force and uniform conphase contact velocity. In the latter case the mixed boundary value problem is circumvented by using a discretized model to find the force distribution. The theoretical values of surface mobility for a circular area with uniform conphase contact velocity are compared to experimental measurements made on a simulated infinite plate.

1. INTRODUCTION

Vibration isolators are used to attenuate the transmission of structural acoustic power from machinery sources and supporting structures. The simplest approach to the design and selection of isolators is based on ensuring that the lowest natural frequency of the system is well below the forcing frequencies from machinery sources. In this simple approach, the mobilities above and below the isolator, that is, the mobilities of the foundation and the machine, are rarely taken into account.

More sophisticated analysis methods take into account the behaviour of the isolator element over a range of frequencies. Examples of this are the blocked transfer function [1] and the four-pole parameter description of isolators [2]. Expressions for the efficiency of isolation involve the isolator properties and the mobilities of the structure above and below the isolator. The structural connections are generally assumed to be point-like, and theoretical or measured values of point mobility are used in an attempt to optimize isolation. For flexural waves in a plate, the use of point mobility assumes that the dimensions of the excitation area are less than approximately one-tenth of a wavelength [3].

The interest associated with high frequency vibration transmission has increased due to increased machine operating speeds and more flexible supporting structures. Consequently, the assumed point-like connection between machine and its support becomes invalid, since the dimensions of the contact area can be comparable to the governing wavelength. Thus, excitations may have complicated spatial distributions and the power transmitted will differ significantly from that occurring when the connection is via a point.

0022–460X/97/160095 + 14 $25.00/0/sv960785

Hammer and Petersson [4, 5] developed the concept of strip mobility based upon complex power and effective mobility approaches. Strip mobility was derived for infinite, homogeneous thin plates excited by either a uniform, conphase force distribution or a uniform, conphase velocity distribution along a finite strip. It was shown that for the two cases investigated, a reduction in power transmission can be gained by using a strip coupling for a given net force.

In this paper the results are presented of a study to determine the surface mobility of large circular contact areas, following on the concepts of Hammer and Petersson [5]. Theoretical results are presented for the two idealized excitation conditions of uniform conphase force and uniform conphase velocity, while experimental results are given for the uniform conphase velocity case. Although a circular contact shape is used in these studies, the general formulations and experimental techniques are applicable to any arbitrary shape.

2. SURFACE MOBILITY

The mobility of a mechanical system, in complex form, is normally defined as

$$\underline{M} = \underline{v}/\underline{F}, \tag{1}$$

where $\underline{F}$ is the excitation force, and $\underline{v}$ is the resulting velocity. (An underscore is used here to denote the complex representation of quantities such as force, velocity and mobility. In the context of machinery isolation, $\underline{F}$ and $\underline{v}$ act in the same direction and nominally at the same point on the foundation or machine; hence the mobility is referred to as a point mobility or driving point mobility.)

By using the driving point mobility the power supplied to the mechanical system may be readily evaluated. Instantaneously, the power supplied is the product of the force and the velocity. Using complex notation, the instantaneous power P_{inst}, can be expressed as

$$P_{inst} = [\mathrm{Re}\ \{\underline{F}\, e^{j\omega t}\}] \cdot [\mathrm{Re}\ \{\underline{v}\, e^{j\omega t}\}]. \tag{2}$$

If the complex quantities F and v are replaced by

$$\underline{F} = F_{re} + jF_{im} \qquad \text{and} \qquad \underline{v} = v_{re} + jv_{im}$$

then

$$P_{inst} = (F_{re} \cos \omega t - F_{im} \sin \omega t)(v_{re} \cos \omega t - v_{im} \sin \omega t). \tag{3}$$

The time averaged power, P, gives the net power flow into the structure over time. Taking a time integral of equation (3) one obtains the expression [3]

$$P = 0{\cdot}5\ \mathrm{Re}\ \{\underline{F}\underline{v}^*\}. \tag{4}$$

Substituting for the input mobility into equation (4), one obtains

$$P = 0{\cdot}5|F|^2\ \mathrm{Re}\ \{\underline{M}\}, \tag{5}$$

where $|\underline{F}|^2 = \underline{F}^*\underline{F}$. Note in the above that the phase of the mobility represents the phase difference between the force and the velocity at the point of contact, whereas the time averaged power is purely real.

It has been shown by Cremer *et al*. [3] for flexural waves in plates, that when the force acts on an area with characteristic dimension less than one-tenth of the governing wavelength in the plate, then the mobility is adequately determined from the total force and velocity at that location. This result was obtained by Cremer *et al*. [3] by considering an asymptotic solution to the case of a circular excitation region acted upon by a uniform

conphase force distribution. In effect, they have used the complex power method, described below, but restricted their results to asymptotic solutions for either very small or very large excitation areas. They note that one may reduce the power input provided by a given net force by distributing this force over as large an area as possible.

When the exciting force is distributed over an area which is large relative to a wavelength, it is useful to define the concept of surface mobility, M^s, in order to relate the exciting force distribution to the time averaged power input to the structure. Note that in this case the phase difference between the local force and velocity will vary from point to point over the contact surface, and hence only the real part of the surface mobility has physical meaning in that it can be used in expressions for the time averaged power, such as

$$P = 0{\cdot}5|F|^2 \,\mathrm{Re}\,\{M^s\}. \tag{6}$$

In equation (6), the power into the structure is related to the net magnitude of the force, $|F|$, where force is interpreted as the net force over the contact area. For this reason, only the real part of the surface mobility needs to be considered, since the imaginary part has no physical meaning.

Two definitions of surface mobility can be formulated, one based on time averaged input and the other based on effective mobilities. These are used in this paper to determine the mobility of circular contact regions of arbitrary size. For convenience, the two surface mobilities are designated as M^{sp} and M^{se} respectively.

2.1. TIME AVERAGED POWER DEFINITION

Consider the stress, $\sigma(x, y, t)$, and velocity, $v(x, y, t)$, distributions over the contact area, S, shown schematically in Figure 1. These stress and velocity distributions can be represented as spatially varying complex phasors, $\underline{\sigma}(x, y)$ and $\underline{v}(x, y)$, where

$$\sigma(x, y, t) = \mathrm{Re}\,\{\underline{\sigma}(x, y)\,\mathrm{e}^{\mathrm{j}\omega t}\} \qquad \text{and} \qquad v(x, y, t) = \mathrm{Re}\,\{\underline{v}(x, y)\,\mathrm{e}^{\mathrm{j}\omega t}\}. \tag{7}$$

The time averaged power transferred through the contact area is given by the integral

$$Q = \tfrac{1}{2}\,\mathrm{Re}\left\{\int_S \underline{\sigma}^*(x, y)\underline{v}(x, y)\,\mathrm{d}s\right\} \tag{8}$$

and the total contact force over the area is given in complex form by

$$\underline{F} = \int_S \underline{\sigma}(x, y)\,\mathrm{d}s. \tag{9}$$

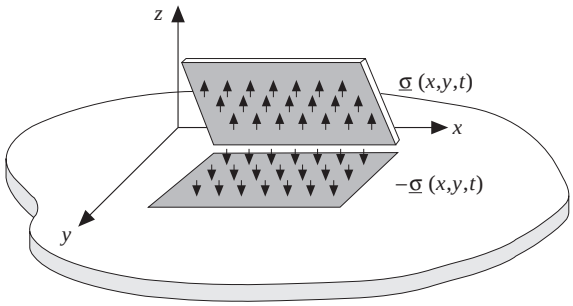

Figure 1. A schematic of a large contact area.

Using the definition for the time averaged power in equation (5), the real part of the area mobility, Re $\{\underline{M}^{sp}\}$, defined on the basis of the power transmitted, can be obtained as

$$\text{Re}\,\{\underline{M}^{sp}\} = \frac{2Q}{|F|^2} = \frac{1}{|F|^2}\,\text{Re}\left\{\int_S \underline{\sigma}^*(x, y)\underline{v}(x, y)\,\mathrm{d}s\right\}. \tag{10}$$

2.2. EFFECTIVE MOBILITY APPROACH

For power transmission in multi-point coupled systems, the concept of effective point mobility may be used [4]. The contact surface can be considered to consist of N contact points. The response at the ith contact point, due to the forces at all points, is called the effective point mobility, and is given by

$$\underline{M}_i^e = \frac{\underline{v}_i}{\underline{F}_i} = \frac{\sum_{j=1}^{N} \underline{M}_{ij} \cdot \underline{F}_j}{\underline{F}_i}, \tag{11}$$

where $\underline{M}_{ij}$ is the transfer mobility between points i and j.

If the contact points are continuously distributed over an area S, the effective point mobility, $\underline{M}^e$, at the point (x_i, y_i) is

$$\underline{M}^e(x_i, y_i) = \frac{\int_S \underline{M}(x_i, y_i \mid x_j, y_j)\underline{\sigma}(x_j, y_j)\,\mathrm{d}x_j\,\mathrm{d}y_j}{\underline{\sigma}(x_i, y_i)}. \tag{12}$$

The total time averaged power transferred through the contact area is

$$Q = \tfrac{1}{2}\int_S |\underline{\sigma}(x_i, y_i)|^2 \cdot \text{Re}\,(\underline{M}^e(x_i, y_i))\,\mathrm{d}s, \tag{13}$$

and so the real part of the surface mobility based upon the effective point mobility is given by

$$\text{Re}\,\{\underline{M}^{se}\} = \frac{\int_S |\underline{\sigma}(x_i, y_i)|^2 \cdot \text{Re}\,(\underline{M}^e(x_i, y_i))\,\mathrm{d}s}{|\int_S \underline{\sigma}(x_i, y_i)\,\mathrm{d}s|^2}. \tag{14}$$

Implementation of the above development requires the specification of the force distribution at the interface. This task is complicated by the fact that the dimensions of the contact area are comparable to the governing wavelength of the support and by the contact conditions between the machine and the support.

3. ASSUMPTIONS AND GOVERNING EQUATIONS

Valuable insight into the behaviour of practical plate-like supporting structures, which have finite dimensions, may be gained by considering the plate as infinite and homogeneous [6]. In the following analyses, losses are neglected, the plate vibrations are assumed to be pure bending and the plate thickness is assumed to be small compared to the governing wavelength.

The equation for the forced bending of the plate is

$$\Delta\Delta\underline{v} - k^4\underline{v} = \frac{\mathrm{j}\omega\underline{\sigma}(x, y)}{B}. \tag{15}$$

The solution of this is a zero-order Hankel function of the second kind.

$$\underline{v}(x, y) = \iint \underline{\sigma}(x, y) \cdot M_0 \cdot \Pi(kr)\, \mathrm{d}x\, \mathrm{d}y, \tag{16}$$

where M_0 is the ordinary point mobility of an infinite plate and

$$\Pi(kr) = \mathrm{H}_0^{(2)}(kr) - \mathrm{H}_0^{(2)}(-\mathrm{j}kr). \tag{17}$$

Using the asymptotic expansion for $\mathrm{H}_0^{(2)}(kr)$, $kr \gg 1$, the far field velocity distribution is

$$\underline{v}(x, y) = \frac{M_0\sqrt{2}}{\sqrt{\pi kr}}\, \mathrm{e}^{\mathrm{j}\pi/4} \iint_S \underline{\sigma}(x, y)\, \mathrm{e}^{-\mathrm{j}kr}\, \mathrm{d}x\, \mathrm{d}y. \tag{18}$$

4. UNIFORM, CONPHASE FORCE DISTRIBUTION

The surface mobility of the infinite plate excited by a uniform conphase force distributed over the circular contact area will be derived using the time averaged power and effective mobility approaches.

4.1. TIME AVERAGED POWER

For a uniform force distribution over the contact area, of radius a, the far field velocity at a radius X is [13]

$$\underline{v}(X) = \sigma_0 \pi a^2 \frac{\sqrt{2}}{\sqrt{\pi kX}} M_0 \frac{2\mathrm{J}_1(ka)}{ka}\, \mathrm{e}^{-\mathrm{j}kX + \mathrm{j}\pi/4}. \tag{19}$$

The power flow through the circumference in the far field is [3]

$$\mathrm{Re}\,[Q] = c_b 2\pi R\rho h|v|^2 = \tfrac{1}{2} M_0 |\sigma_0 \pi a^2|^2 \left[\frac{2\mathrm{J}_1(ka)}{ka}\right]^2 \tag{20}$$

and is equal to the real part of the power transfer through the contact area, $S = \pi a^2$.

Thus the real part of the surface mobility is

$$\mathrm{Re}\,(\underline{M}^s) = M_0 \left[\frac{2\mathrm{J}_1(ka)}{ka}\right]^2, \tag{21}$$

which shows that the surface mobility depends on the Helmholtz number, ka.

In Figure 2 is shown the variation of the real surface mobility, normalized with respect to M_0, as a function of Helmholtz number. It can be seen that the real part of the surface mobility decreases rapidly as the Helmholtz number increases above 1. For $ka = 1$ the surface mobility is approximately 70% of the ordinary point mobility, while for $ka = 2$ the surface mobility is only 5% of the point mobility. The real part of the surface mobility also exhibits oscillatory behaviour, with minima occurring at $ka = 3{\cdot}8317$, $7{\cdot}0156$, $10{\cdot}1735 \ldots$. As ka increases, the difference between consecutive minima tends to π. These minima occur when the diameter of the contact region is close to a multiple of the wavelength of the plate vibration.

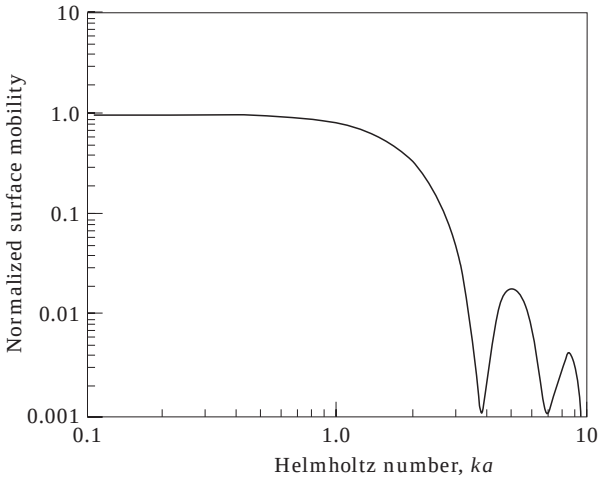

Figure 2. Normalized surface mobility versus Helmholtz number for uniform, conphase force over a circular area.

4.2. EFFECTIVE MOBILITY

For a circular contact area the effective mobility at (R, φ), for a uniform conphase force is

$$\underline{M}^e(R, \varphi) = a^2 \int_0^1 \int_0^{2\pi} \underline{M}(R, \varphi/\rho, \theta)\rho \, \mathrm{d}\rho \, \mathrm{d}\theta, \tag{22}$$

where R and ρ are the radial distances of the response point and the force, non-dimensionalized by the contact radius a.

For an infinite, homogeneous plate the transfer mobility can be written as [3]

$$\underline{M}(R, \varphi/\rho, \theta) = M_0 \Pi(kr) = M_0(\mathrm{H}_0^{(2)}(kr) - \mathrm{H}_0^{(2)}(-\mathrm{j}kr)), \tag{23}$$

where $r = a\sqrt{\rho^2 + R^2 - 2\rho R \cos(\varphi - \theta)}$.

The real part of this transfer mobility can be approximated as

$$M(R, \varphi/\rho, \theta) = M_0 \mathrm{J}_0(kr), \tag{24}$$

which gives the real part of the effective point mobility as

$$\mathrm{Re}\{\underline{M}^e(R, \varphi)\} = a^2 \int_0^1 \int_0^{2\pi} M_0 \mathrm{J}_0(kr)\rho \, \mathrm{d}\rho \, \mathrm{d}\theta. \tag{25}$$

The effective point mobility is independent of the angular location, φ. The variation of the normalized effective point mobility for different values of R is plotted in Figure 3. The mobility curves coincide at $ka = 3{\cdot}8317$, which is the first minimum for the first order Bessel function of the first kind. For $ka < 3{\cdot}8317$, the effective point mobility is greatest at the centre. For $3{\cdot}8 < ka < 6{\cdot}8$, the effective point mobility at the centre point is negative, implying that power is transmitted back into the contact patch from the plate.

In Figure 4 is shown the variation of the real part of the effective point mobility with R, for different values of ka. For $ka = 5$ the effective mobility is negative for $0 < R < 4$, implying a large area in which power is circulating within the contact area and not

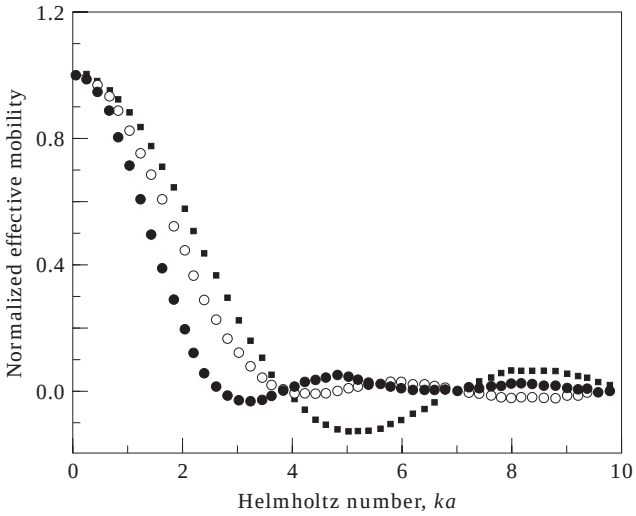

Figure 3. Effective point mobility (constant force) versus Helmholtz number for different values of R. ■, $R = 0{\cdot}0$; ○, $R = 0{\cdot}5$; ●, $R = 0{\cdot}9$.

transmitted into the far field. In Figures 3 and 4 it is indicated that for values of $ka > 3{\cdot}8$ there will be areas in which power circulates within the plate and the contact area. For $ka = 8$ the region of negative power flow occurs for $0{\cdot}32 < R < 0{\cdot}65$.

The time averaged input power is

$$Q = \frac{a^2}{2} |\sigma|^2 \int_0^1 \int_0^{2\pi} \mathrm{Re}\,(\underline{M}^e(R, \varphi)) R \, \mathrm{d}R \, \mathrm{d}\varphi. \tag{26}$$

Thus the real part of the surface mobility, normalized by the ordinary point mobility, is

$$\mathrm{Re}\,(\underline{M}^s) = \frac{M_0}{\pi^2} \int_0^1 \int_0^{2\pi} \left[\int_0^1 \int_0^{2\pi} \mathrm{J}_0(kr) \rho \, \mathrm{d}\rho \, \mathrm{d}\theta \right] R \, \mathrm{d}R \, \mathrm{d}\varphi. \tag{27}$$

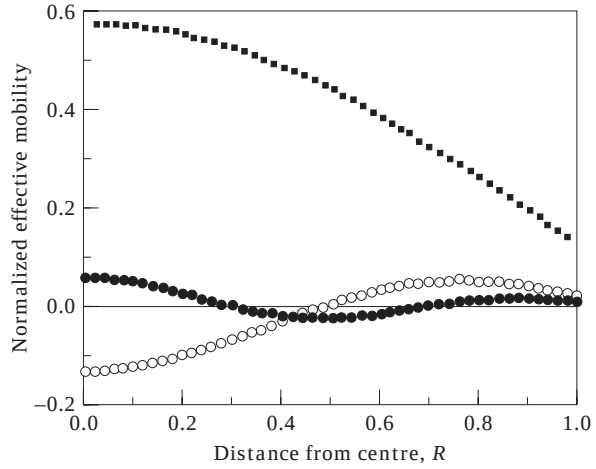

Figure 4. Effective mobility versus R at different Helmholtz numbers. ■, $ka = 2$; ○, $ka = 5$; ●, $ka = 8$.

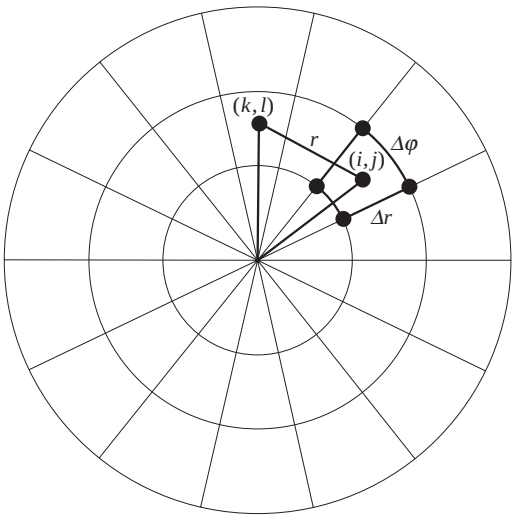

Figure 5. A schematic of the discretized model of a circular area.

Numerical integration of equation (27) produced results to within a few percent of those obtained using the complex power approach shown in Figure 2.

5. UNIFORM CONPHASE VELOCITY

For a prescribed velocity field over the contact area it is necessary to determine the force distribution in order to derive the surface mobility. In this section a discretized model is used to determine the force distribution, the effective point mobility and hence the surface mobility.

The velocity distribution over the plate is given by equation (16). The boundary conditions for a uniform conphase velocity over the contact area are

$$\underline{\sigma}(x, y) = 0, \quad \text{for } \sqrt{x^2 + y^2} > a \qquad \text{and} \qquad \underline{v}(x, y) = \underline{v}(0, 0), \quad \text{for } \sqrt{x^2 + y^2} \leqslant a. \quad (28)$$

In this paper a discretized model, shown in Figure 5, is used to find an approximation to the stress distribution.

The circular contact region is subdivided into $L \times N$ sub-regions, with constant intervals $\Delta r = a/L$ and $\Delta\varphi = 2\pi/N$, in the radial and tangential directions, respectively. If the sub-regions are small enough, then the forces in each sub-region can be approximated by the effect of a point force

$$\underline{P}_{kl} = \int_{\rho_1}^{\rho_2} \int_{\varphi_1}^{\varphi_2} \underline{\sigma}(\rho, \varphi)\, \mathrm{d}\rho\, \mathrm{d}\varphi. \quad (29)$$

This net force is assumed to act at the centre of the sub-region.

The velocity at the centre of sub-region (k, l) due to the force acting at the centre of sub-region (i, j) is

$$\underline{v}(k, l) \mid (i, j) = M_0 \underline{P}_{ij} \Pi(kr),$$

$$r = (a/L)\sqrt{(k - 0{\cdot}5)^2 + (i - 0{\cdot}5)^2 - 2(k - 0{\cdot}5)(i - 0{\cdot}5)\cos(j - l)\Delta\varphi}. \quad (30)$$

The velocity at the centre of sub-region (k, l) due to the forces at the centres of all the sub-regions is found by superposition:

$$\underline{v}(k, l) = M_0 \sum_{i=1}^{L} \sum_{j=1}^{N} \underline{P}_{ij} \Pi(kr), \tag{31}$$

which can also be expressed in matrix form

$$\{\underline{v}\} = [\underline{T}]\{\underline{P}\} \tag{32}$$

where $\{\underline{v}\}$ and $\{\underline{P}\}$ are column vectors of length equal to the number of sub-regions and $[\underline{T}]$ is a square matrix. Due to symmetry conditions the force and velocity distributions will be functions only of the radial co-ordinate only. Thus equation (32) can be reduced to

$$\{\underline{v}\} = [\underline{U}]\{\underline{P}'\}, \tag{33}$$

where $\{\underline{v}\}$ and $\{\underline{P}'\}$ are now vectors of length L, and $[\underline{U}]$ is a square matrix of order $L \times L$.

After this reduction only L linear equations need to be solved for L unknowns. Once the force vector $\{\underline{P}'\}$ is determined, one has the force distribution over the whole contact region, since $\underline{P}(i + j \times L) = \underline{P}'(i)$ for $i = 1$ to L, and $j = 1$ to $N - 1$.

The total force is written as

$$\underline{F} = \sum_{i=1}^{L \times N} \underline{P}(i) = N \sum_{i=1}^{L} \underline{P}'(i). \tag{34}$$

The total time averaged power input over the excitation region is, retaining the matrix

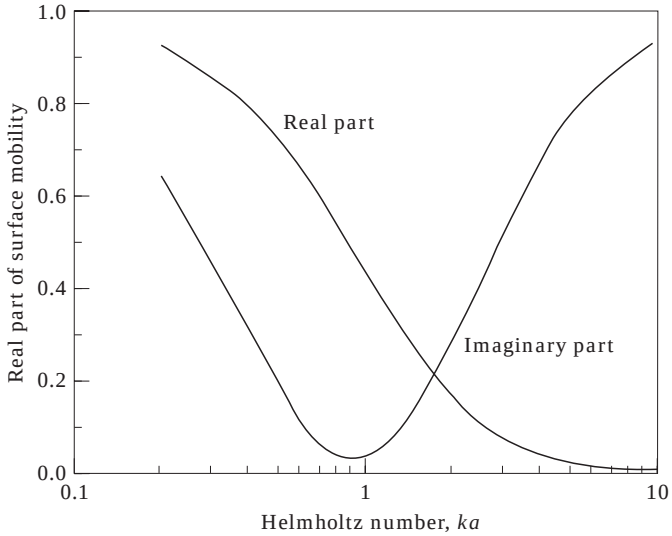

Figure 6. Normalized surface mobility versus Helmholtz number for a uniform conphase velocity over a circular contact area.

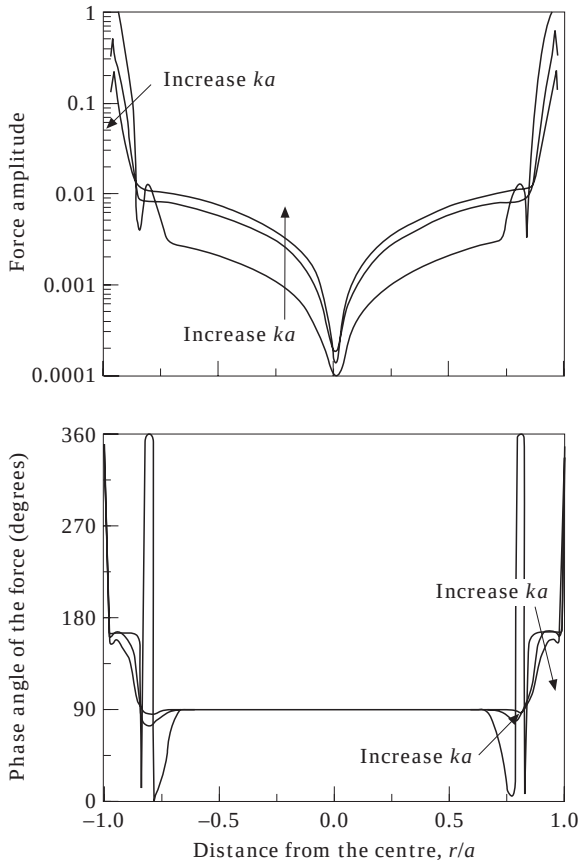

Figure 7. The spatial variation of the force distribution for $ka = 1$, 3 and 5.

notation,

$$Q = \tfrac{1}{2}\,\mathrm{Re}(\{\underline{P}\}^{\mathrm{T}}([\underline{T}]\{\underline{P}\})^*) \qquad \text{or} \qquad Q = \tfrac{1}{2}\,\mathrm{Re}\left\{\sum_{i=1}^{L\times N}\sum_{j=1}^{L\times N}\underline{P}(j)(\underline{P}(i)\underline{T}(i,j))^*\right\} \tag{35}$$

Hence the real part of the surface mobility on the time averaged power basis for the circular contact area is

$$\mathrm{Re}\,\{\underline{M}^{se}\} = \frac{\displaystyle\sum_{i=1}^{L\times N}\sum_{j=1}^{L\times N}\underline{P}(j)(\underline{P}(i)\underline{T}(i,j))^*}{\left|\displaystyle\sum_{i=1}^{L\times N}\underline{P}(i)\right|^2}. \tag{36}$$

An iterative procedure was used to calculate the surface mobility. Starting with $L_1 \times N_1$ discrete elements the force distribution and hence the surface mobility was calculated. The procedure was then repeated for $(L_1 + 1) \times (N_1 + 1)$, $(L_1 + 2) \times (N_1 + 2)$ etc., elements, until the difference between successive determinations was less than 0·1%. The real part of the normalized surface mobility is shown in Figure 6. The real part of the surface mobility and hence the active power transmitted decreases as ka increases. However, unlike

the uniform, conphase force distribution, there is no oscillatory behaviour at high Helmholtz numbers.

The effective point mobility for the centre point of a sub-region, i, is

$$\underline{M}^{se}(\rho_i) = \sum_{j=1}^{L \times N} \frac{\underline{T}(i,j)\underline{P}(j)}{\underline{P}(i)}, \tag{37}$$

which is independent of the angular co-ordinate. The spatial variation of the force for different Helmholtz numbers is shown in Figure 7, while the spatial variation of the effective mobility for different Helmholtz numbers is shown in Figure 8. The maximum effective mobility occurs at the centre, and there is a rapid decrease in the effective mobility occurs at the centre, and there is a rapid decrease in the effective mobility as ka increases. For $r < 0{\cdot}7a$ the phase of the effective mobility is constant and independent of ka. However, towards the edge of the contact area, there are significant phase variations.

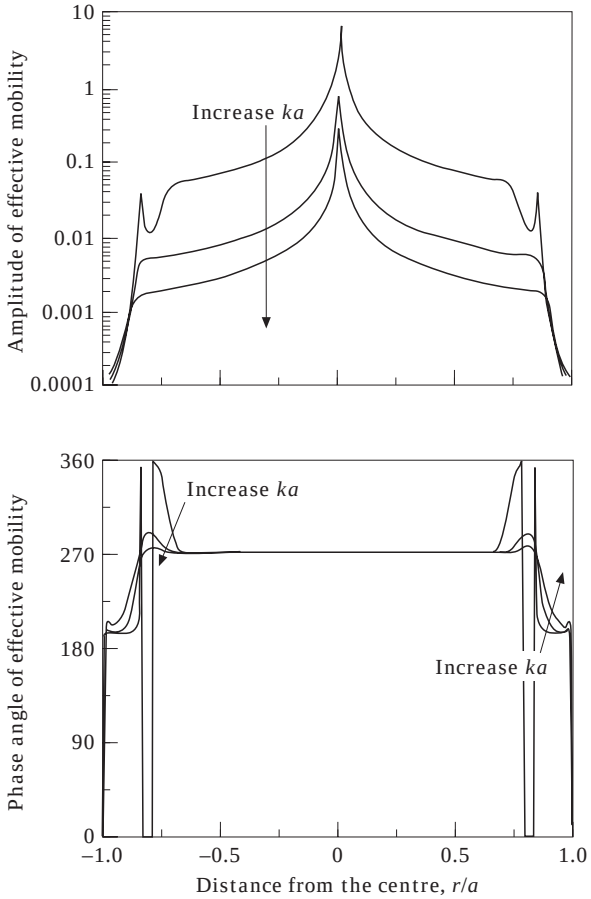

Figure 8. The spatial variation of the normalized effective mobility for $ka = 1$, 3 and 5.

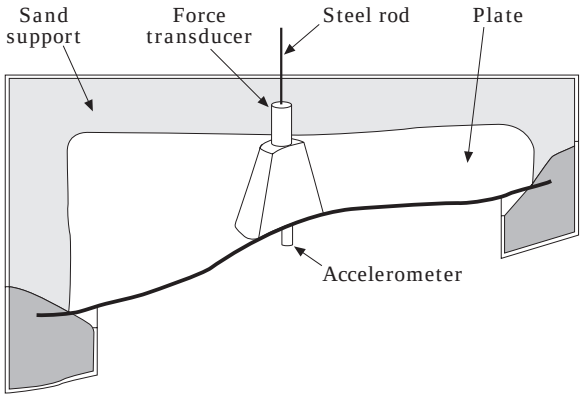

Figure 9. A schematic of the measurement set-up for uniform contact velocity.

6. EXPERIMENTAL DETERMINATION OF SURFACE MOBILITY FOR UNIFORM VELOCITY DISTRIBUTION

Driving point mobility is normally determined by measuring the input force and the response velocity, using either an impedance head or a force transducer and an accelerometer, and correcting for any transducer mass loading effects. The measurement of surface mobility is, however, much more difficult, as in the general case the exact force and velocity distribution over the contact area is not known.

For the particular case of a uniform, conphase velocity distribution over the contact area, the response velocity may be measured directly, and the surface mobility determined from equation (1), after correcting the force measurement for any mass loading. A close approximation to a uniform velocity distribution over the contact area will occur when an isolator with a stiff base is mounted on a relatively flexible plate. In this series of experiments this condition was achieved by gluing an aluminium cone to a 1 mm thick plate measuring $2{\cdot}4\text{ m} \times 1{\cdot}2\text{ m}$. The edges of the plate were embedded in sand to approximate anechoic boundary conditions and hence simulate an infinite plate; see Figure 9. The cone was glued to the plate centre and driven by a Brüel and Kjaer type 4810 shaker attached through a type 8200 force transducer, with the response measured by a Brüel and Kjaer 4374 accelerometer. Brüel and Kjaer type 2635 charge amplifiers were used for all

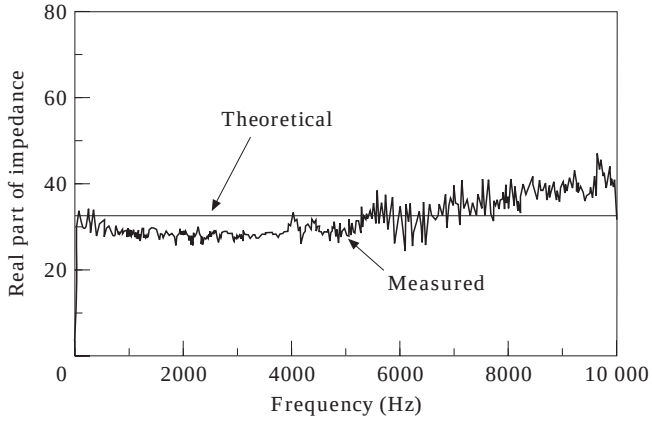

Figure 10. The point impedance of the test plate.

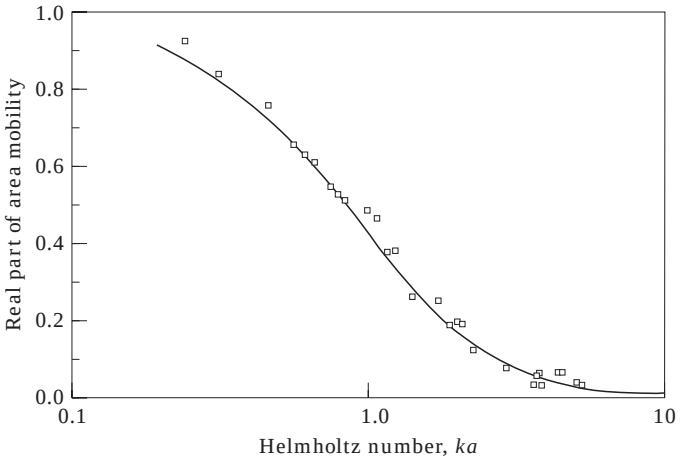

Figure 11. A comparison of experimental (□) and theoretical (——) results for constant velocity contact.

signal conditioning and spectral analysis was performed using a Hewlett Packard 35665A analyzer. Broadband random excitation was used during the experiments.

The input mobility was determined by dividing the response velocity at the centre of contact area by the input force, with the force corrected for the mass loading of the cone, accelerometer and attachment hardware. The distribution of the velocity over the contact area was measured to ensure that it was uniform. Measurements of the plate driving point impedance via a *point* connection were made to assess the quality of the anechoic terminations; see Figure 10. Measurements of the surface mobility were made for four different contact patch sizes, of 25 mm, 50 mm, 100 mm and 150 mm diameter. The surface mobility measurements are compared to the theoretical curve for uniform velocity distribution in Figure 11.

The theoretical value of the point impedance of a 1 mm thick infinite plate, calculated using $z = 8\sqrt{(B\rho h)}$, is 32·968 Ns/m. The measured point, as shown in Figure 10, is in good agreement with the theoretical figure, indicating that the plate models an infinite plate well.

The surface mobility data for the cones shows excellent agreement with the theoretical curves. It clearly demonstrates the decrease in mobility as the Helmholtz number increases. In Figure 11 it is shown that the results for surface mobility between cones are consistent, and that the quality of the agreement between the theoretical and experimental data is not dependent upon the cone size.

7. CONCLUDING REMARKS

Using both the complex power approach and the effective mobility approach, the surface mobility for a circular contact area on an infinite plate has been developed. Two cases, of uniform conphase force and of uniform conphase velocity at the interface, have been considered. For the latter case a discretized model was used to derive the force distribution over the contact region. It is shown for both conditions that the surface mobility decreases rapidly as the Helmholtz number increases. This implies that there is a reduction in the power transmitted through the large contact area compared to a point contact, for the same net force. The magnitude of the effective point mobility for both uniform force and uniform velocity cases varies greatly over the contact region and is largest at the centre.

Experimental measurements of the surface mobility for a uniform velocity distribution are presented and show excellent agreement with the theoretical results.

REFERENCES

1. J. W. VERHEIJ 1982 *Ph.D. Thesis*, *Institute of Applied Acoustics TNO-TH*, *Delft*. Multi-path sound transfer from resiliently mounted shipboard machinery.
2. J. D. DICKENS, C. J. NORWOOD and R. G. JUNIPER 1993 *Proceedings of the Australian Acoustical Society Annual Conference*, *Glenelg*, *Australia*. Four pole parameter characterisation of isolator acoustic transmission performance.
3. L. CREMER, M. HECKL and E. E. UNGAR 1988 *Structure-borne Sound*. Berlin: Springer-Verlag; second edition.
4. P. HAMMER and B. PETERSSEN 1989 *Journal of Sound and Vibration* **129**, 119–131. Strip excitation, part 1: strip mobility.
5. P. HAMMER and B. PETERSSEN 1989 *Journal of Sound and Vibration* **129**, 132–142. Strip excitation, part 2: upper and lower bounds for the power transmission.
6. E. SKUDRZYK 1958 *Journal of the Acoustical Society of America* **30**, 1140–1152. Vibrations of a system with a finite or an infinite number of resonances.